Strathprints Institutional Repository

Laser-driven x-ray and neutron source development for industrial applications of plasma accelerators

C M Brenner[1], S R Mirfayzi[3], D R Rusby[1,2], C Armstrong[1,2], A Alejo[3],
L A Wilson[1], R Clarke[1], H Ahmed[3], N M H Butler[2], D Haddock[1],
A Higginson[2], A McClymont[1], C Murphy[4], M Notley[1], P Oliver[1], R Allott[1],
C Hernandez-Gomez[1], S Kar[3], P McKenna[2] and D Neely[1]

[1] Central Laser Facility, STFC, Rutherford Appleton Laboratory, Didcot, Oxon, OX11 0QX, UK
[2] Department of Physics, SUPA, University of Strathclyde, Glasgow G4 0NG, UK
[3] Centre for Plasma Physics, Queen's University Belfast, Belfast BT7 1NN, UK
[4] Department of Physics, University of York, York YO10 5DD, UK

E-mail: ceri.brenner@stfc.ac.uk

Abstract

Pulsed beams of energetic x-rays and neutrons from intense laser interactions with solid foils are promising for applications where bright, small emission area sources, capable of multi-modal delivery are ideal. Possible end users of laser-driven multi-modal sources are those requiring advanced non-destructive inspection techniques in industry sectors of high value commerce such as aerospace, nuclear and advanced manufacturing. We report on experimental work that demonstrates multi-modal operation of high power laser-solid interactions for neutron and x-ray beam generation. Measurements and Monte Carlo radiation transport simulations show that neutron yield is increased by a factor ~2 when a 1 mm copper foil is placed behind a 2 mm lithium foil, compared to using a 2 cm block of lithium only. We explore x-ray generation with a 10 picosecond drive pulse in order to tailor the spectral content for radiography with medium density alloy metals. The impact of using >1 ps pulse duration on laser-accelerated electron beam generation and transport is discussed alongside the optimisation of subsequent bremsstrahlung emission in thin, high atomic number target foils. X-ray spectra are deconvolved from spectrometer measurements and simulation data generated using the GEANT4 Monte Carlo code. We also demonstrate the unique capability of laser-driven x-rays in being able to deliver single pulse high spatial resolution projection imaging of thick metallic objects. Active detector radiographic imaging of industrially relevant sample objects with a 10 ps drive pulse is presented for the first time, demonstrating that features of 200 μm size are resolved when projected at high magnification.

Keywords: laser, acceleration, plasma, applications

1. Introduction

High power laser-driven acceleration of electrons and ions from solid targets is a productive area of study in plasma beam physics, in part due to the extreme physics of generating ultra-high gradient accelerating fields through the interaction of a

relativistically intense laser pulse with an ionised medium. It is also a thriving area of research due to the application potential of pulsed, bright, micro-sized accelerating structures in generating sources of x-rays [1], ions [2] and neutrons [3] for use in imaging, heating and probing scientific or industrial test samples [4, 5]. Of the many regimes of plasma acceleration discussed in the literature, the interaction of a short (~ several ps) laser pulse (with irradiance $I_L\lambda^2 > 10^{18}$ W μm^2 cm^{-2}) with a solid foil generating an electron pulse with high peak current (MA) transporting through to the rear surface of the target, has now become a robust and reliable source of ions and x-rays. High energy bremsstrahlung x-rays [1] with beam temperatures up to several MeV are generated when relativistic (hot) electrons, directly accelerated by the laser fields at the target front surface, transport through and interact with the solid material of the foil (see figure 1). Ions are accelerated when a portion of the hot electron beam escapes through the rear surface of a foil, establishing TV/m electric fields that ionise and accelerate ions in the forward direction and pull back the remaining portion of the hot electron beam. Protons, compared to heavier target ions, accelerated from contaminant layers on the target surface are the dominant signal in the measured beam through this acceleration scheme, due to having the highest charge-to-mass ratio. Proton beams generated from this description of rear-surface plasma sheath acceleration [6] (commonly known as target normal sheath acceleration, TNSA) have broadband, Maxwellian distribution spectra, with the majority of the proton beam energy in the energy band 1–10 MeV, for picosecond, PW-scale laser drivers. Reproducible proton beams generated using simple thin foils are easily obtained with spectra that extend to ~30 MeV [2]. Recent measurements of the conversion efficiency of laser energy into the proton beam have demonstrated 15% [7] under double pulse irradiation [8] with a 1 ps laser and 4% with a 30 fs laser [9], both of which are very promising observations for their use in applications requiring high doses.

The main limitation of industrial application of these sources is the design infrastructure of PW-scale laser systems. Their low ($\ll$Hz) repetition rate, large installation footprint and cost of electrical and manpower to run and maintain them thus limits them mostly to nationally managed laboratories at present. Yet, with the recent development of diode-pumped high energy systems [10], capable of many Hz repetition rate and significant light generation efficiency, the reality of high-power laser-driven radiation sources available outside of national laboratory infrastructure is fast approaching.

The spectra of laser-driven x-rays and protons from solid foils currently achievable and reported in the literature by many groups across various laser systems are reproducible and suitable for demonstration experiments in which their applicability for a variety of end-uses can be examined. We report here on laser-solid interaction experiments that utilise qualities and characteristics of bright, broadband, high energy proton beams for neutron generation and x-rays for radiography applications relevant to industrial users. The demand from industrial applications for laser-driven x-ray and neutron beams is explored in section 2, ahead of introducing the experimental arrangement in which the Vulcan laser is

employed for multi-modal beam generation. In section 4 we consider proton-induced neutron generation and explore the effect of a stacked design for the proton convertor target. In section 5 we exploit the tunable quality of these beams for radiograph imaging and demonstrate spectral validation of laser-driven x-ray emission—an important consideration for applications development. Finally, we present a short portfolio of laser-driven x-ray radiograph images that demonstrate the unique and highly applicable nature of these sources for non-destructive inspection of large industrial objects. These demonstration experiments are crucial for guiding continuing research into establishing mechanisms for control and optimisation, indicating the avenues that should receive more effort in our goal to fully harness and broaden their application potential. This work complements the breadth of applications demonstrated with laser acceleration from gas targets [11–13] and strengthens the multi-modal source offering of laser drivers.

2. Industrial applications

Laser-driven bremsstrahlung sources have been measured since the early days of laser plasma experiments [14, 15]. Along with the observation of relativistic electron acceleration in solid foils came highly directional, energetic and small emission area x-ray beams, capable of imaging through large and dense objects [1, 16]. These pulsed x-rays are well suited for radiography and non-destructive testing applications in security and high value sectors, such as aerospace, nuclear and advanced manufacturing. Their high brightness and energy, short duration and $\ll$1 mm^2 emission area point source make them unique compared to their commercially available counterparts, cathode ray flash x-ray tubes and linac sources, which cannot achieve all of these qualities in a single source. Much experimental work has been conducted to characterise x-ray emission from solid targets across a variety of laser systems [17, 18], as well as radiography demonstration of the imaging qualities of the beams [19, 20]. The ability to control and tune the spectral content of these x-rays beams using laser pulse parameters makes this generation mechanism an attractive prospect for use in a variety of complex imaging environments. The added benefit of single shot image acquisition extends the application environment to include dynamic imaging and testing of test objects in damage-inducing conditions where large standoff distances are necessary and improves inspection techniques by shortening exposure times required for high quality imaging.

Utilising laser-driven protons for neutron generation by transporting the beam into a convertor material to induce (p,n) reactions is fast emerging as a key application of sheath accelerated beams [3]. Pulsed neutron sources are an important experimental resource for non-destructively probing the lattice and atomic structure of materials and have a user base that it is both scientifically and industrially motivated. Synchrotron-accelerated proton beams driven into spallation targets and reactors are the main sources of neutrons used by the research community for science exploration. However, there is growing demand from security, aerospace and
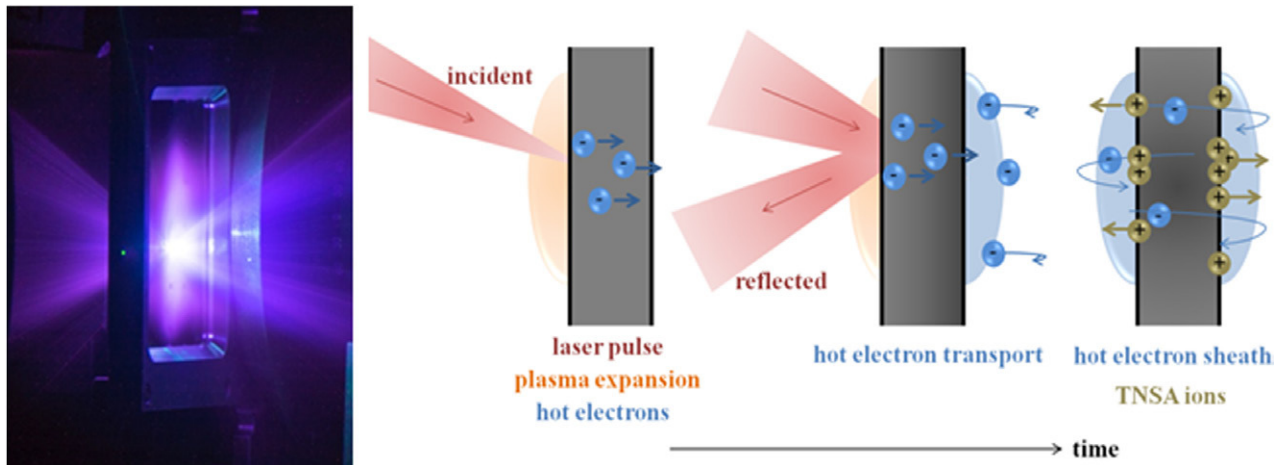
Figure 1. Photograph of the laser interaction with a solid foil (left) alongside schematic of the sheath acceleration mechanism.
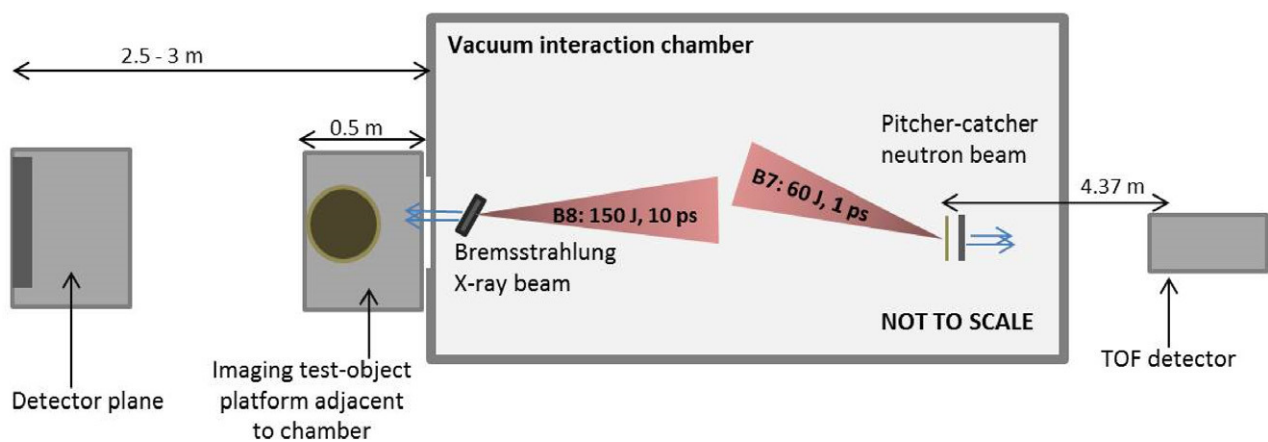

Figure 2. Experimental layout demonstrating multi-modal generation using the Vulcan laser beams.

manufacturing industries to obtain neutron sources for routine inspection and imaging techniques in the private sector. Laser-driven sources offer high brightness, short pulse generation mechanisms that could be used for these techniques, with a substantial decrease in infrastructure footprint and even the potential for portability with improvements in high power laser systems. Laser-driven sources generate fast neutrons (>MeV energies) with high flux rates that are also considered useful for investigating materials under neutron bombardment for fusion reactor designs [21]. Experimental observations using proton capture (p,n) reactions in convertor targets such as lithium, boron and beryllium and x-ray driven photoneutron generation in copper are demonstrating neutron beams with significant brightness of the order 10^{8-10} n sr^{-1} per pulse [3, 22–24]. Coupling a large amount of energy into the laser-proton driver is a key characteristic for this application, more so than the intensity distribution or the spectral shape of the proton beam. For example, industrial neutron radiography, a technique considered an essential tool in material science and advanced engineering, requires ~10^6 n cm^{-2} of thermal energy range at the sample/detector plane [25] to generate a high quality image of neutron transmission through different materials. Imaging with fast neutrons is likely to require much higher neutron numbers to generate contrast in a transmission image, due to their lower capture efficiency in the detector

medium. It is worth considering that the prompt generation of high energy x-rays also presents challenges in utilising the neutron beams for applications, as it greatly supersedes over the neutron signal and causes detector saturation. Roth *et al* [23] employed the significant time of flight separation of x-ray and neutron pulses at large distances from the source to gate-out the x-ray flash and obtain a neutron radiograph image, detected using an array of scintillating fibres coupled to a CCD chip. Fast decay-time scintillator diagnostics [26, 27] are clearly an important requirement for applications of laser-driven neutron beams.

3. Multi-modal radiation generation experimental set-up using high power lasers

The generation of multi-modal beams from a single driving system is a highly appealing feature of high power laser-solid sources. An experiment was carried out using the Vulcan laser at the Central Laser Facility [28] to enable dual mode investigation of neutron and x-ray beam generation from laser irradiated solid foil targets. Two beams of the Vulcan laser, B7 and B8, were used in back-to-back formation (see figure 2) to deliver 62 ± 6 J in 1.0 ± 0.2 ps pulses (intensity $I_L \sim 8 \times 10^{19}$ W cm^{-2}) and 150 ± 15 J in 10 ± 2 ps pulses (intensity $I_L \sim 2 \times 10^{19}$ W cm^{-2}), respectively. Both B7 and
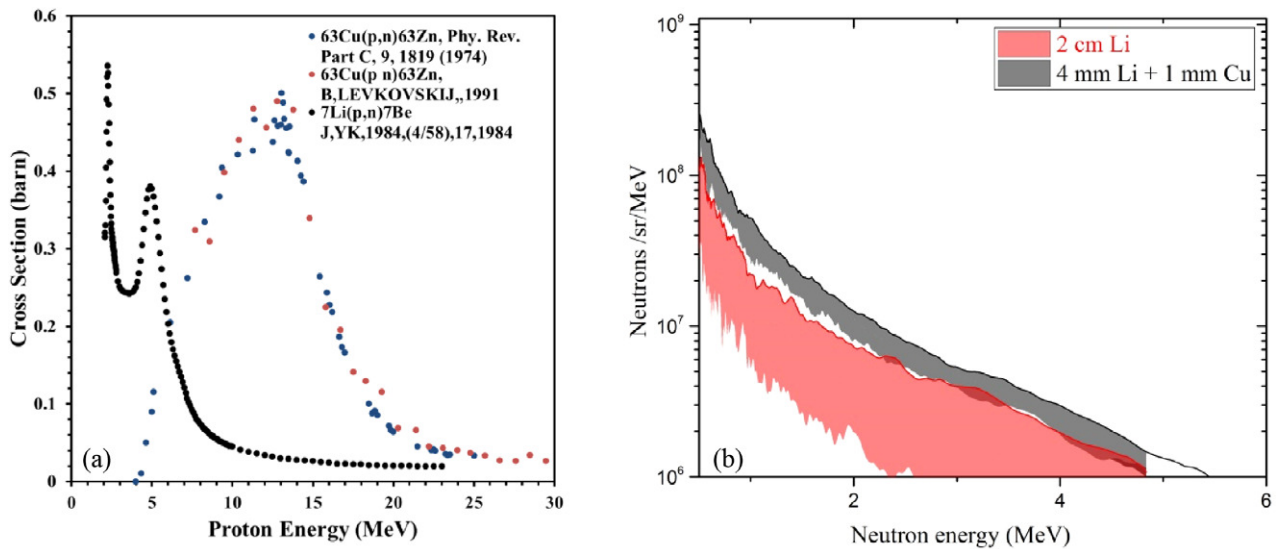
Figure 3. (a) Neutron generation cross sections as a function of proton energies impinging on lithium and copper and (b) measured neutron spectra for the two convertor designs.

B8 are p-polarised, 1.054 μm wavelength laser pulses and were used to drive electron acceleration at the front surface of solid foil targets by focusing the beams with a F/3 off-axis parabola to spots of 5×7 μm^2 area at 20 degrees incidence. B7 was used to drive sheath acceleration of protons from the rear surface of 10 μm thick gold foils into neutron convertor foils spaced 0.5 cm from the source foils, in a 'pitcher-catcher' configuration. Smooth, round proton beams with energy up to 20 MeV and characteristic sheath-acceleration spectrum [7] were consistently measured 5 cm from the source with stacks of Radiochromic film [29], during shots prior to the installation of the catcher targets. B8 was used to drive bremsstrahlung x-ray generation from hot electron transport through tantalum foils of thickness 100 μm. The x-rays then passed through a 2 mm thick aluminium vacuum port and were used to image a variety of test-objects via absorption contrast radiography.

## 4. Laser-driven neutron beam enhancement

Designing a convertor target that utilises all of the beam content is the optimal approach to neutron generation from plasma sheath acceleration. A convertor design made up of layered stacks of material can enable photo-neutron emission to be induced by high energy laser-driven x-rays with >MeV energy [24] alongside proton-driven reactions [3]. Furthermore, using a stack configuration takes advantage of the broadband distribution of the proton beam by considering the Bragg peak deposition curve of protons and knowing the proton energy for which there is a peak in the (p.n) cross-section for a given material. The effect of convertor design on neutron generation via laser-driven acceleration from gold planar foils of thickness 10 μm was investigated experimentally and numerically using the FLUKA Monte Carlo simulation code. The neutron beams were detected by absolutely calibrated, fast-decay scintillating crystals located at a distance 4.37 metres from the source, aligned along the target normal laser axis. The neutron beam spectra were deconvolved using a time-of-flight

method that compares neutron time of arrival to the prompt high energy x-ray signal detected [26].

The convertor holder was placed directly behind the rear surface of the gold foils at a distance of 0.5 cm. A dual-layer convertor made up of 4 mm thick lithium (Li^7) and 1 mm thick copper (with lithium closest to target rear surface) was compared against a design with a 2 cm thick block of lithium (Li^7). Neutrons are generated in lithium through the $Li^7(p,n)Be^7$ reaction with the cross-section for the reaction peaking at 2–3 MeV proton energy [3]. The addition of copper in this new stack design convertor is expected to enhance the neutron generation by utilising the threshold for $Cu^{63}(p,n)^{63}Zn$ reactions at 4 MeV and a peak in the cross-section for the reaction at ~10 MeV protons (see figure 3(a)).

Neutron spectra from repeat measurements where the laser interaction and 'pitcher' target conditions are held constant but the catcher configuration is varied are shown in figure 3(b). The optimum spectrum for each pitcher-catcher configuration is shown in bold and the associated shaded regions indicate spectral measurements collected from the repeat shots, indicating the margin of reproducibility. These measurements demonstrate that using the Li + Cu convertor generates an increase by a factor ~2 in the number of neutrons generated in the forward direction along target normal across the whole spectrum of 1–5 MeV neutrons. The Li + Cu catcher spectra are also more reproducible on a shot-to-shot consideration, indicating that the beam generation is much more stable. A Monte Carlo modelling software for calculating stopping ranges of ions in matter, SRIM [30], indicates that protons with energy >13 MeV will transmit through the 4 mm lithium foil, depositing the majority (>80%) of their energy within the copper foil. The laser-driven pitcher-catcher neutron production was simulated using the FLUKA Monte Carlo code [31] to compare expected neutron yield from the two catcher designs. Protons of energy >13 MeV were transported through the catchers and the energy spectra of neutrons generated on axis were compared.
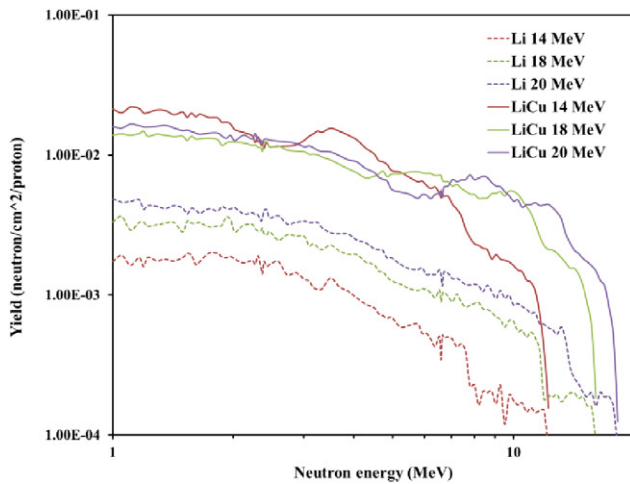
Figure 4. Neutron spectra generated using the FLUKA code by simulating protons of a given energy (shown in the graph legend) transporting through the two catcher target designs, Li and LiCu.

Figure 4 shows that the additional neutron generation mechanism from $Cu^{63}(p,n)^{63}Zn$ reactions with protons >13 MeV results in an enhanced neutron yield (by a factor 2–3) for neutrons with energy <5 MeV, in good agreement with our experimental observation. x-rays of energy >10 MeV will also be generated from the laser interaction with the gold foil target and will contribute to the neutron number enhancement. However, with only 1 mm of copper in use and the low photon density of x-rays at this energy, the photoneutron reaction rate is very small compared to the $Cu^{63}(p,n)^{63}Zn$ reaction rate. The addition of these neutron generation reactions in copper to those induced in the lithium foil gives rise to an enhanced neutron flux that appears more stable against the effect of shot-to-shot fluctuations in the proton beam, compared to using only a thick block of lithium in which the $Li^7(p,n)Be^7$ reaction is the main generation mechanism. This demonstrates the benefit of designing convertor targets that make use of all the neutron generation reactions that are achievable with the emission of a multi-species, broadband radiation beam.

5. Laser-driven x-ray beams with 10 ps driver

5.1. Spectral tuning via laser and target parameters

The combination of high energy, single-shot acquisition and short pulse exposure for high resolution x-ray radiography of large, dense objects provided in a tunable laser-driven system is an attractive prospect for industrial users that wish to employ this technique on a range of components and materials under various conditions. It is also important that a small emission area is maintained, so as to achieve ≪1 mm spatial resolution at high magnification to meet industrial imaging requirements. In order to obtain good absorption contrast with the test objects materials in this present study, made of aluminium and titanium alloys, the hot electron spectrum was tuned to reduce the amount of high energy (>500 keV) photons generated. High energy x-rays transmit through these materials with low absorption and therefore contribute significant image noise.

The laser intensity was reduced by increasing the Vulcan laser pulse duration from <1 ps to 10 ± 2 ps. Using this laser parameter as the control parameter ensures that the maximum laser energy available is delivered over the smallest area for absorption into a x-ray generating hot electron beam. Decreasing the laser intensity also has the effect of reducing the divergence of the hot electron beam, as shown by Green *et al* [32], which should help to minimise the x-ray emission area. The transport of a hot electron beam generated by a 10 ps drive laser is more complex than for short pulse bunches, since this duration is longer than the characteristic growth time for self-generated magnetic field structures around the transporting hot electron beam that act to induce filamentation, beam breakup, collimation or deflection about the laser target normal axis. Scott *et al* [33] used double-pulse irradiation under similar conditions to those used here to demonstrate that a collimating magnetic field structure was active ~6 ps after a hot electron beam was generated. Within the duration of the rising edge and at the peak of a 10 ps laser pulse, collimation of the hot electrons is therefore expected, resulting in minimum emission area of the highest energy x-rays. However, at later times hot electron beam break-up can occur which will degrade the angular profile of x-ray emission. Modelling all of the physics of hot electron transport on timescales of 1–10 ps is computationally challenging, but is necessary to fully establish the benefits and side-effects of using the laser pulse duration as a control parameter for x-ray emission and will be the focus of future work.

A tantalum foil target was deployed, since high atomic number materials generate the highest yield of x-ray photons for a given input hot electron beam [34]. The target thickness was determined by considering the stopping range of hot electrons in tantalum and a population with temperature 600 keV generated by the laser intensity, I_L ~ 2×10^{19} W cm^{-2}. The Beg hot electron scaling [35] with intensity was used here, since the direction of x-ray emission was primarily along the target normal axis. This is indicative of the resonance absorption process being the dominant laser electron heating factor, conditions under which the Beg scaling was derived. The stopping distance of the majority of the electron density in this distribution is 300 μm path length. This path length can be reached in three passes through a 100 μm thick target since the hot electrons will undergo refluxing between the surfaces, with two of the passes contributing to forward emission. Employing the effect of refluxing to reduce the target thickness from 300 μm down to 100 μm also helps to reduce the amount of x-rays absorbed in the dense target material as they propagate forward. However, it is noted that transverse spreading of the hot electron beam when significant refluxing is occurring during the laser pulse duration [36] has been shown to increase the x-ray source size, particularly for targets of thickness <100 μm. This simple analytical approach for determining target thickness is in agreement with the findings of Fiorini *et al* [34], in which they determine optimum mass thicknesses for photon yield by incorporating refluxing of hot electrons in a FLUKA Monte Carlo transport model.
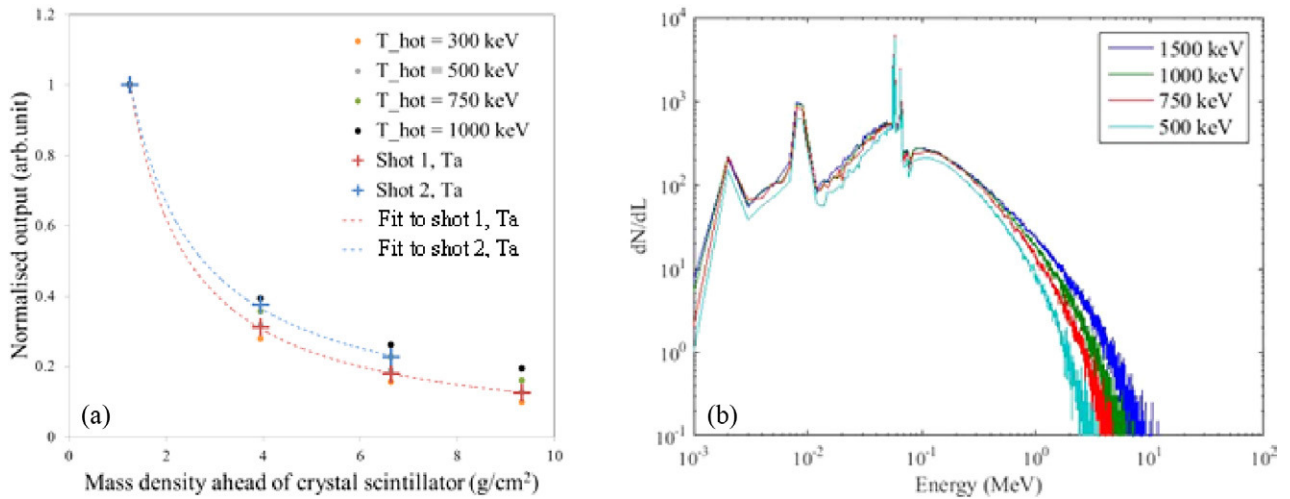
Figure 5. (a) Measured output signal of the x-ray scintillator spectrometer, compared to modelled output from various hot electron temperature distributions transporting through Ta foil and (b) x-ray spectra generated by Geant4 simulations of hot electron populations with various temperatures transporting through solid foils.

5.2. Spectrometer measurement of x-ray emission

The ability to verify spectral content of laser-driven bremsstrahlung sources is an important process in the development of predictive models that can tailor the laser and target conditions required for each imaging application. A scintillator-based, high-energy x-ray spectrometer has been developed [37] for on shot monitoring of x-ray emission from laser-solid interactions. The spectrometer uses an array of scintillating crystals that absorb x-rays and emit visible light proportional to the absorbed energy, which is coupled to a CCD chip. In order to deconvolve the x-ray spectrum, a Monte Carlo simulation code Geant4 [38] is employed to calculate bremsstrahlung spectra output generated by a variety of relativistic Maxwellian electron temperature distributions transporting through a solid foil. Previous studies [39, 40] have investigated the result on bremsstrahlung generation of hot electrons being driven back and forth through solid foil targets by the refluxing effect of sheath fields establishing instantaneously on the target surfaces. Refluxing increased the overall yield of forward x-ray emission but does not significantly change the energy distribution, therefore it has not been included in these present simulations. By multiplying the simulated x-ray spectra by the response function of the detector, expected output spectra can be compared to measured output from the spectrometer.

The spectrometer was positioned along the target normal axis and sampled the x-ray emission from two shots in which the laser intensity on the target was 8.5×10^{18} W cm^{-2}. Normalised values of the measured output were then compared to simulated values using the process described above (see figure 5(a)). The best fit to the measured output was simulated using electron temperatures of 650 ± 150 keV, the variation in temperature for these repeat shots being due to fluctuations in laser energy and pulse duration, indicated by the reproducibility margins stated within section 3. Figure 5(b) displays example x-ray spectra generated from a range of simulations in which the hot electron temperature is similar to that inferred

from the deconvolution method used here. Increasing the hot electron temperature further increases the maximum photon energy but does not have a significant effect on the photon flux, demonstrating a tunability of spectral content by tuning the hot electron population with laser parameters. Wilson *et al* [39] and Coury *et al* [41] have studied the effect of increasing laser focal spot size on x-ray emission as an alternative spectral tuning parameter. It is worth noting that along with spectral content, monitoring of the angular distribution [42] and flux of emitted radiation is of high importance in order to feed the development of predictive imaging models. The methods described by Gray *et al* [43] and Rusby *et al* [44] for measuring emitted electrons are a suitable approach to this end.

5.3. Radiography demonstration

For dynamic imaging of large objects, the small ($\ll 1$ mm) emission area of high flux and energy x-ray pulses from a laser-driven plasma interaction offer a distinct advantage over conventional sources in which one or more of these properties are often sacrificed to achieve another. To employ laser-driven x-rays within an industrial setting and meet the expectations of non-expert end-users interested in high resolution and single-shot imaging through large dense objects also requires the development of active detectors, which can deliver instant digital images under >1 Hz acquisition operation.

Radiography of a variety of test objects was carried out demonstrating the high quality imaging properties of x-ray pulses generated during laser-solid interactions with the Vulcan laser at the Rutherford Appleton Laboratory. BAS-SR image plate detector film was used to measure the x-rays after transmission through the test objects in order to produce radiographs. A newly developed 2D active scintillator-based detector, constructed of Thalium doped Caesium Iodide (CsI) pixels of width 500 μm × 500 μm and thickness 1 cm, optically coupled to CCD chips, with full working area of 30×30 cm^2, was also fielded. The active detector provides instant images
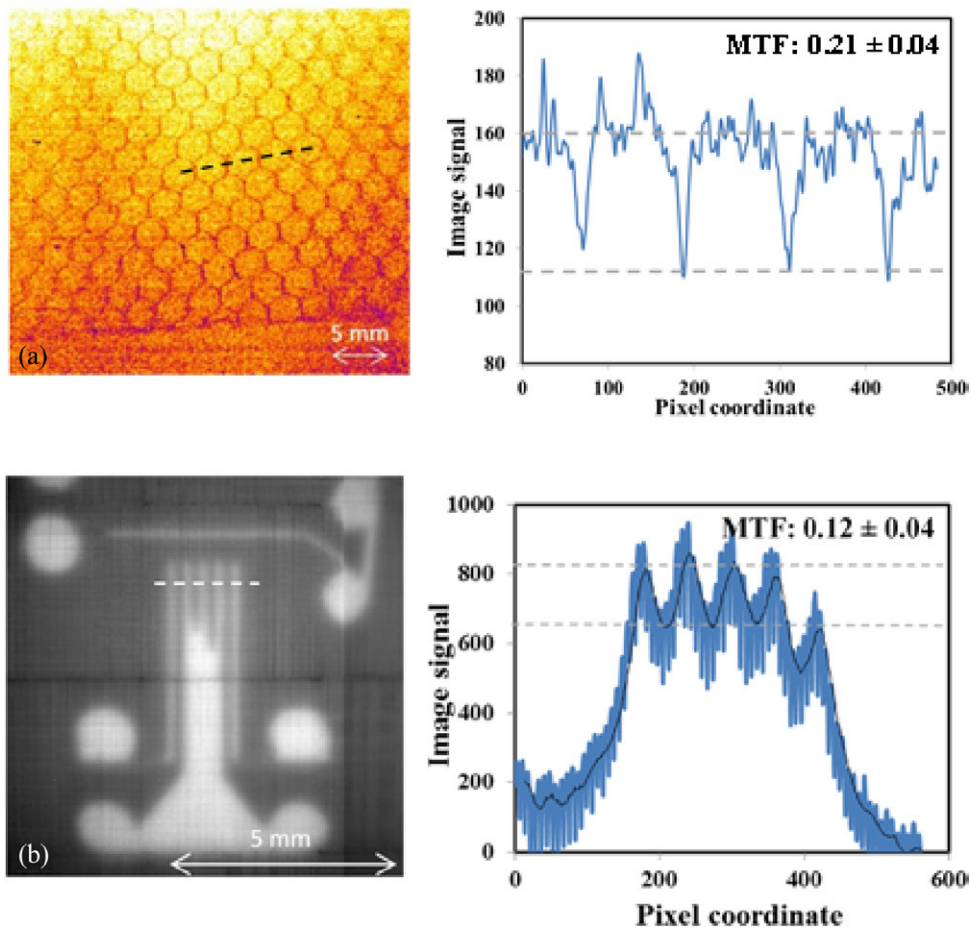
Figure 6. (a) Radiograph imaging of a titanium object with internal fine structure using image plate detector in contact (magnification 1) alongside a line profile of the area indicated by the dashed line and (b) radiograph of a 5 mm thick tungsten plate wire cut with 200 μm width slits imaged using the CsI detector under high magnification (magnification 10), alongside a line profile of the area indicated by the dashed line.

compared to the traditional IP film, for which digitising the signal at high resolution can take up to 1 h for a single 20 cm × 40 cm piece. A spatial resolution test object was produced from 5 mm thick, 100 mm × 100 mm tungsten plate, designed to highly attenuate x-rays with energy <500 keV. The plate was wire-cut to produce resolution test pattern slits in the plate, of various widths down to 200 μm.

All of the test objects were positioned outside the vacuum interaction chamber, in the plane of the laser axis, at different distances from the detectors in order to image at various magnification factors. Contact radiography (magnification 1) of a test object constructed of 3 cm thick titanium alloy, containing pure titanium structure of thickness 1 cm and width ~200 μm, demonstrates that a single-pulse exposure of laser-driven x-rays is sufficient to resolve the contrast in attenuation of x-rays through an object with low density and complex structure within a higher density background (see figure 6(a)). The modulation transfer function (MTF), a quantitative description of image contrast where perfect MTF = 1, deduced from the line-out shown in figure 6(a) is 0.21 ± 0.04, indicating good projection of the object attenuation contrast onto the detector plane. With zero distance between the test object and the image plate the image spatial resolution is given by the resolution of the detector readout, which is ~50 μm in this case.

Therefore, the 200 μm width features are easily resolved when using contact IP radiography and is a result that could be obtained with most conventional x-ray sources. However, the unique capability of laser-driven sources is in the delivery of high-resolution single-pulse projection imaging. At high magnification, during which the smallest features are projected over many pixels of the detector, the spatial resolution of an image is defined by the source emission area. In order to test the spatial resolution for projection imaging with this laser-driven source a high magnification radiograph of the 5 mm thick tungsten resolution plate was taken. Figure 6(b) shows an image of 200 μm width gaps in the tungsten plate, projected with magnification factor 10 onto the active detector panel (pixel size 500 μm), that are visible with MTF = 0.12 ± 0.04 when obtained with single pulse exposure.

With applications in mind, this demonstrates that features of much less than 1 mm size within a thick metallic background are visible under single-shot radiography acquisition when using laser-driven bremsstrahlung emission from laser-solid interactions coupled to an instant readout active detector located at a large standoff distance to the test object. This is a crucial demonstration of laser-driven x-rays for non-destructive testing and industrial radiography, as it indicates unique capability compared to conventional technology.
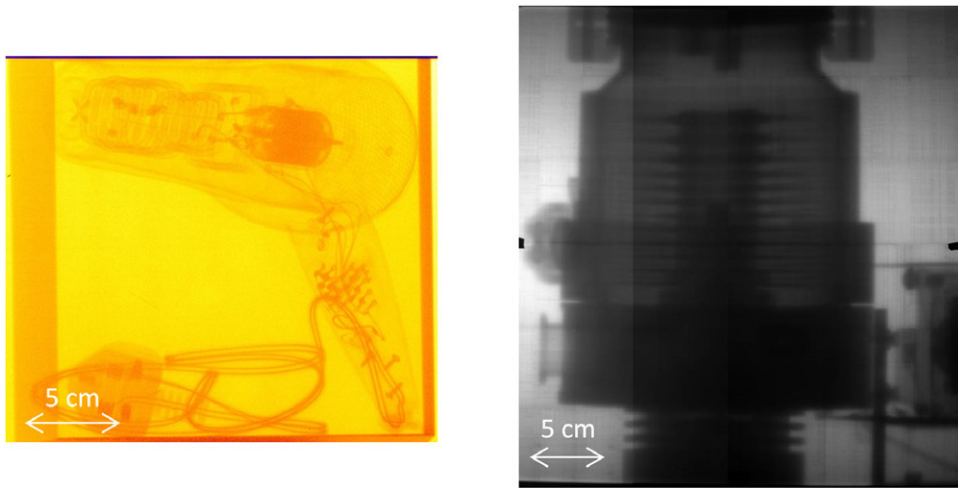
Figure 7. Contact radiography of a hairdryer within a 1 mm thick Aluminium box recorded on image plate (left) and turbomolecular vacuum pump using the CsI active detector (right).

To obtain structure visibility in single-shot radiographs of low density materials (e.g. plastic and aluminium) at extreme standoff distances from the source, image plate is required due to its superior dynamic range and high sensitivity to x-rays with energy <60 keV, compared to the active detector. Figure 7 demonstrates contact radiography of a test object positioned at >45 degrees to the laser axis, at a distance >2.5 m from the source, indicating high image quality even when utilising the low flux 'wings' of the Guassian angular distribution. The large working area of the active CsI array detector was employed to capture a wide field-of-view single-shot contact radiograph of a turbomolecular vacuum pump (figure 7), further demonstrating that laser-driven x-rays have the brightness and small source emission area for imaging full-scale components at high resolution ($\ll 1$ mm) in a single short-pulse exposure.

These demonstration examples indicate that laser-driven sources are already capable of high quality imaging that exceeds conventional source capability and that with further optimisation of the beam spectral content, flux and detectors along with emission area characterisation, this radiography method can only improve.

6. Summary and discussion

In summary, we have demonstrated an increase in laser-driven neutron yield of a factor ~2 across the neutron energy range 1–5 MeV by utilising a stacked proton catcher design and presented tuning of the x-ray spectral emission for single-pulse high spatial resolution projection imaging of industrially relevant objects while using a newly-developed active detector screen. These source development and detector demonstration results are an important step-forward in realising laser-driven beams for applications in areas such as non-destructive and non-invasive testing and imaging for industry users whereby their short pulse duration, small emission area and high brightness makes them unique compared to conventional alternatives.

Laser-driven proton beams were utilised for neutron generation by transporting them into a convertor material that makes use of the many neutron generation reactions that are achievable with the emission of a multi-species, broadband energy radiation and particle beam. A stack convertor design, made of lithium and copper foils, was found to enhance and stabilise the neutron spectrum along the forward target normal axis, as a proof of principle demonstration. In this present work, a neutron density ~10^7 n cm^{-2}/pulse at 5 cm from the source is demonstrated and yet this was achieved without fully optimising conditions for laser proton generation and convertor design. This neutron flux bodes well for laser-generation use in industrial applications, especially when coupled to high shot rate laser technology, such as the DiPOLE 10 Hz laser [10].

Laser-driven bremsstrahlung x-ray beams are generated from 100 μm thick tantalum foils, using 10 ps duration laser pulses to tune the emission for radiography of medium-density metallic test objects. A scintillator-based x-ray spectrometer is used to deconvolve the spectrum of the x-ray emission, presenting a vital step forward for on-shot beam monitoring required for industrial applications development. 200 μm width slits in a 5 mm thick tungsten plate are clearly visible when radiographed with single pulse exposure at high magnification onto an active detector screen, thus utilising the high brightness and small emission area characteristics of the source. This is a crucial demonstration for non-destructive testing and industrial radiography and displays unique imaging capability. Resolution with MTF ~ 0.1 of the test grid features suggests an upper limit of the source size to be 200 μm, obtained for conditions of 10 ps laser pulse irradiating 100 μm thick Ta foils at best (smallest) focus position. This compares favourably against a 350 μm source size measurement made with 10 ps, 1 kJ laser pulses irradiating 2 mm thick Ta foils [20]. Source sizes of <200 μm down to 87 μm [36] have been measured from laser-solid interactions, but with shorter laser pulse lengths of 1 ps and 0.6 ps, respectively. Further work on front surface generation and hot electron transport is needed to deduce whether <100 μm source sizes can be achieved with lasers of pulse length > 1 ps.

One of the most appealing characteristics of laser-driven beams of radiation is their tunable and multi-modal operation, controlled by simply changing laser pulse and target conditions. It is clear that detailed descriptions are required of how the key beam properties such as the spectral content, flux and uniformity of these bright and directional beams vary with laser properties, in order to establish the most suitable mechanisms and approaches for control for industrial applications.

Acknowledgments

References

[1] Edwards R D *et al* 2002 *Appl. Phys. Lett.* **80** 2129
[2] Daido H *et al* 2012 *Rep. Prog. Phys.* **75** 056401
[3] Yang J M *et al* 2004 *J. Appl. Phys.* **96** 6912
[4] Borghesi M *et al* 2008 *Plasma Phys. Control. Fusion* **50** 124040
[5] Ledingham K W D and Galster W 2010 *New J. Phys.* **12** 045005
[6] Wilks S C *et al* 2001 *Phys. Plasmas* **8** 542
[7] Brenner C M *et al* 2014 *Appl. Phys. Lett.* **104** 081123
[8] Markey K *et al* 2010 *Phys. Rev. Lett.* **105** 195008
[9] Green J S *et al* 2014 *Appl. Phys. Lett.* **104** 214101
[10] Mason P D *et al* 2015 *Appl. Opt.* **54** 4227–38
[11] Gizzi L A *et al* 2015 *Nucl. Instrum. Methods Phys. Res.* B **355** 241–5
[12] Albert F *et al* 2014 *Plasma Phys. Control. Fusion* **56** 084015
[13] Najmudin Z *et al* 2014 *Phil. Trans. R. Soc.* A **372** 20130032
[14] Kephart J F *et al* 1974 *Appl. Phys. Lett.* **25** 108
[15] Columbant D *et al* 1973 *J. Appl. Phys.* **44** 3524
[16] Norreys P *et al* 1999 *Phys. Plasmas* **6** 2150
[17] Ben-Ismail A *et al* 2011 *Appl. Phys. Lett.* **98** 264101
[18] Chen C D *et al* 2013 *Phys. Plasmas* **20** 052703
[19] Glinec Y *et al* 2005 *Phys. Rev. Lett.* **94** 025003
[20] Courtois C *et al* 2011 *Phys. Plasmas* **18** 023101
[21] Perkins L J *et al* 2000 *Nucl. Fusion* **40** 1
[22] Lancaster K L *et al* 2004 *Phys. Plasmas* **11** 3404
[23] Roth M *et al* 2013 *Phys. Rev. Lett.* **110** 044802
[24] Pomerantz I *et al* 2014 *Phys. Rev. Lett.* **113** 184801
[25] Kockelmann W *et al* 2007 *Nucl. Instrum. Methods Phys. Res.* A **578** 421–34
[26] Mirfayzi S R *et al* 2015 *Rev. Sci. Instr.* **86** 073308
[27] Green J *et al* 2011 *Proc. SPIE* **8079** 807919
[28] Hernandez-Gomez C *et al* 2006 *J. Phys. IV France* **133** 555–9
[29] Nurnberg F *et al* 2009 *Rev. Sci. Inst.* **80** 033301
[30] Ziegler J F *et al* 2010 *Nucl. Instrum. Methods Phys. Res.* B **268** 1818–23
[31] Ferrari A *et al* 2005 FLUKA: a multi-particle transport code (program version 2005) No. INFN-TC-05-11 http://citeseerx.ist.psu.edu/viewdoc/summary?doi=10.1.1.393.4720
[32] Green J S *et al* 2008 *Phys. Rev. Lett.* **100** 015003
[33] Scott R H H *et al* 2012 *Phys. Rev. Lett.* **109** 015001
[34] Fiorini F *et al* 2013 *Laser Part. Beams* **32** 233–241
[35] Beg F N *et al* 1997 *Phys. Plasmas* **4** 447
[36] Compant La Fontaine A *et al* 2013 *Phys. Plasmas* **20** 123111
[37] Rusby D R *et al* 2014 *CLF Ann. Rep.* **1**
[38] Agostinelli S *et al* 2003 *Nucl. Instrum. Methods Phys Res.* A **506** 250–303
[39] Quinn M N *et al* 2011 *Plasma Phys. Control. Fusion* **53** 025007
[40] Wilson L A *et al* 2015 *Laser Part. Beams* submitted
[41] Coury M *et al* 2013 *Appl. Phys. Lett.* **100** 074105
[42] Meadowcroft A L and Edwards R D 2012 *IEEE Trans. Plasma Sci.* **40** 1992
[43] Gray R J *et al* 2011 *Appl. Phys. Lett.* **99** 171502
[44] Rusby D R *et al* 2016 *J. Plasma Phys.* **81** 475810505